14. R. L. Folk, *Petrology of Sedimentary Rocks*, Hemphill Publishing (Austin, TX, 1980).
15. R. Greeley *et al*., *Science* **305**, 810 (2004).
16. H. Y. McSween *et al*., *Science* **305**, 842 (2004).
17. M. P. Golombek *et al*., *Lunar Planet. Sci.* [CD-ROM], abstract 2185 (2004).
18. K. E. Herkenhoff *et al*., *Science* **305**, 824 (2004).
19. H. J. Melosh, *Impact Cratering*, Oxford Univ. Press (New York, 1989).
20. J. A. Grant, P. H. Shultz, *J. Geophys. Res.* **98**, 11025 (1993).
21. M. Hurst, M. P. Golombek, R. Kirk, *Lunar Planet. Sci.* [CD-ROM], abstract 2068 (2004).
22. R. E. Arvidson *et al*., *Science* **305**, 821 (2004).
23. W. K. Hartmann, J. Anguita, M. A. de la Casa, D. C. Berman, E. V. Ryan, *Icarus* **149**, 37 (2001).
24. W. K. Hartmann *et al*., *Nature* **397**, 586 (1999).
25. F. Horz, M. J. Cintala, W. C. Rochelle, B. Kirk, *Science* **285**, 2105 (1999).
26. J. A. Grant, P. H. Schultz, *J. Geophys. Res.* **98**, 15033 (1993).
27. P. R. Christensen *et al*., *Science* **305**, 837 (2004).
28. S. W. Squyres *et al*., *Science* **305**, 794 (2004).
29. R. P. Irwin, A. D. Howard, T. A. Maxwell, *Lunar Planet. Sci.* [CD-ROM], abstract 1852 (2004).
30. G. Komatsu, V. R. Baker, *J. Geophys. Res.* **102**, 4151 (1997).
31. K. A. Milam *et al*., *J. Geophys. Res.* **108**, 8078 (2003).
32. M. P. Golombek, N. T. Bridges, *J. Geophys. Res.* **105**, 1841 (2000).
33. Research was supported by NASA through the Mars Exploration Rover Project. Our sincere thanks go to the Mars Exploration Rover management, staff, and engineering teams for their outstanding support and operation of Spirit.

Plates Referenced in Article

www.sciencemag.org/cgi/content/full/305/5685/807/DC1

Plates 1, 3, 5, and 9

3 May 2004; accepted 28 June 2004

REPORT

Wind-Related Processes Detected by the Spirit Rover at Gusev Crater, Mars

R. Greeley,[1] S. W. Squyres,[2] R. E. Arvidson,[3] P. Bartlett,[4] J. F. Bell III,[2] D. Blaney,[5] N. A. Cabrol,[6] J. Farmer,[1] B. Farrand,[7] M. P. Golombek,[5] S. P. Gorevan,[4] J. A. Grant,[8] A. F. C. Haldemann,[5] K. E. Herkenhoff,[9] J. Johnson,[9] G. Landis,[5] M. B. Madsen,[10] S. M. McLennan,[11] J. Moersch,[12] J. W. Rice Jr.,[1] L. Richter,[13] S. Ruff,[1] R. J. Sullivan,[2] S. D. Thompson,[1] A. Wang,[3] C. M. Weitz,[14] P. Whelley,[1] Athena Science Team

Wind-abraded rocks, ripples, drifts, and other deposits of windblown sediments are seen at the Columbia Memorial Station where the Spirit rover landed. Orientations of these features suggest formative winds from the north-northwest, consistent with predictions from atmospheric models of afternoon winds in Gusev Crater. Cuttings from the rover Rock Abrasion Tool are asymmetrically distributed toward the south-southeast, suggesting active winds from the north-northwest at the time (midday) of the abrasion operations. Characteristics of some rocks, such as a two-toned appearance, suggest that they were possibly buried and exhumed on the order of 5 to 60 centimeters by wind deflation, depending on location.

In the current environment of Mars, wind appears to be the most frequent agent of surface modification, resulting in albedo patterns that change on time scales as short as a few weeks (*1*). Abundant dune forms, mantles of windblown deposits, and wind-eroded features are seen from orbit in many parts of Mars, including the three previous sites where successful landings have occurred. Understanding the processes that form aeolian (wind-related) features provides insight into the evolution of the martian surface, including rates of erosion and deposition. The Mars Exploration Rover (MER) Spirit landed near the middle of Gusev Crater (*2*–*5*) in a relatively low-albedo zone (*6*) considered to be a track left by the passage of dust devils that removed bright dust to expose a relatively darker substrate (Fig. 1A). Comparison of orbital images taken of the same area from July 2003 to January 2004 show changes in the tracks, indicating that dust devils were recently active.

Here, we describe initial analyses of aeolian features during the first ~90 sols (*7*) of operation. Wind-related features include sediments (some of which are organized into bedforms such as ripples), wind-abraded features on rocks, eroded zones around rock edges, and features generated by the rover during operations that suggest active winds.

The surface at Columbia Memorial Station consists of rocks, regolith, dark granules, and fine-grained material, including dust (*8*, *9*). Patches of red regolith range in size from 0.5 m across to as large as 15 m across. Bonneville (*10*) crater and many of the small depressions, called hollows, are partly filled with regolith deposits. Light-toned material was inferred to be dust, the upper surfaces of some rocks, the rover solar panels, and the Panoramic Camera (Pancam) calibration target (*11*). Although dust grains are too small to be resolved by the Microscopic Imager (MI) (*12*), previous estimates suggest that martian dust is a few micrometers in diameter (*13*, *14*).

An MI image of a regolith patch shows a bimodal size distribution of particles (Fig. 1B) that includes coarse (1 to 3 mm) grains and finer grains smaller than a few hundred micrometers in diameter. Although some coarse grains are subangular, most are rounded, suggesting erosion during transport. We propose that the dark coarse particles are lithic fragments on the basis of their basaltic composition (*16*, *17*) and appearance in the MI images (*18*).

Aprons of granular debris occur as isolated patches on the regolith and around some rocks. For example, the rock Adirondack (*2*) has an encircling debris apron that extends 5 to 20 cm from the edge of the rock. The aprons consist of coarse grains that have spectral properties similar to those of Adirondack and the other basaltic rocks in the area (*11*, *19*). Therefore, some of the more angular coarse-grained material is probably derived

[1]Department of Geological Sciences, Arizona State University, Box 871404, Tempe, AZ 85287–1404, USA. [2]Department of Astronomy, Cornell University, 428 Space Sciences Building, Ithaca, NY 15853–1301, USA. [3]Department of Earth and Planetary Sciences, Washington University, One Brookings Drive, St. Louis, MO 63031–4899, USA. [4]Honeybee Robotics, 204 Elizabeth Street, New York, NY 10012, USA. [5]Jet Propulsion Laboratory, 4800 Oak Grove Drive, Pasadena, CA 91109–8099, USA. [6]Ames Research Center, Moffett Field, CA 94035–1000, USA. [7]Space Science Institute, University of Colorado, Boulder, CO 80301, USA. [8]Center for Earth and Planetary Studies, National Air and Space Museum, Smithsonian Institution, Washington, DC 20560–0315, USA. [9]U.S. Geological Survey, 2255 North Gemini Drive, Flagstaff, AZ 86001–1698, USA.[10]Niels Bohr Institute for Astronomy, Physics, and Geophysics, Center for Planetary Science and Ørsted Laboratory, University of Copenhagen, Universitetsparken 5, DK-2100 Copenhagen, Denmark. [11]Department of Geosciences, State University of New York at Stony Brook, Stony Brook, NY 11794–2100, USA. [12]Department of Earth and Planetary Sciences, University of Tennessee, 1412 Circle Drive, Room 306, Knoxville, TN 37996, USA. [13]Deutches Zentrum für Luft-und Raumfart (German Aerospace Center)–Institute of Space Simulation, Linder Hoene, D-51170 Cologne, Germany. [14]National Aeronautics and Space Administration (NASA) Headquarters, Washington, DC 20546–0001, USA.

*To whom correspondence should be addressed. E-mail: Greeley@asu.edu

from physical weathering of rocks in the area, as suggested for the Mars Pathfinder (MPF) site on the basis of spectral properties (*14*). Although the dark regolith within Bonneville crater was not examined in situ, the regolith has similar aprons on its surface.

Bedforms are common at the site and range in size from 0.1 m long by 0.03 m wide by 0.02 m high to 10 m long by 2 m wide by 0.5 m high. They have wavelengths of 0.06 to 10 m, with the larger bedforms having longer wavelengths. The larger bedforms are only seen within Bonneville crater and on the outer flanks of the crater and can be identified in orbital images. In cross section, most bedforms are slightly asymmetric, with the southeast sides being steeper and higher in albedo than the northwest sides. Thermal infrared spectral emissivity measurements (*16*) across meter-scale bedforms show asymmetry that correlates with the visible-wavelength albedos. The higher albedo southeast slopes show a thermal infrared (IR) signature of dust that is equivalent to the globally homogeneous dust (*20*). Spectra of the lower-albedo northwest-facing slopes suggest the presence of materials compositionally similar to the rocks seen at the site and is attributed to thepresence of particles similar to those composing the debris aprons.

MI images taken on one bedform named

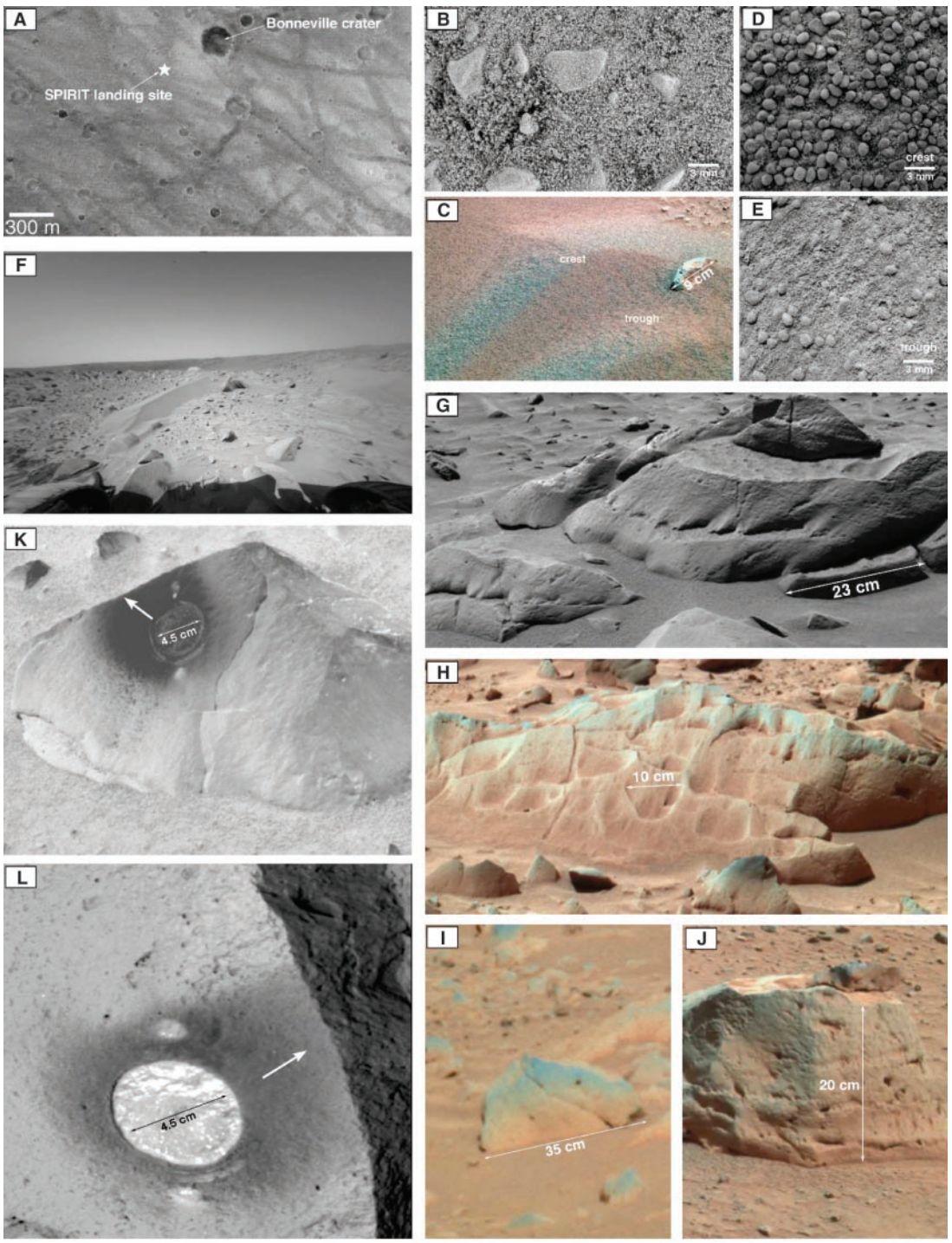

Fig. 1. (**A**) Mars Orbiter Camera (MOC) image R12-01091. View of the Spirit site from orbit showing the Columbia Memorial Station (star) and the impact crater, Bonneville. The relative dark zones are tracks left by the passage of dust devils. One prominent track crosses Bonneville crater. (**B**) MI image, 2M130463156EFF0900P2943M21, of regolith showing large, subangular granules set in smaller, sand-size grains. The spectral properties of the granules suggest that they are lithic fragments. (**C**) Pancam image, 2P129911125FFL0500P2399L2M1, of the ripple, Arena. (**D**) MI image, 2M130001357EFF0506P2953M2M1, of Arena crest, showing well-sorted rounded grains. (**E**) MI image, 2M130001885EFF0506P2943M2M1, of Arena trough zone, showing poorly sorted grains. (**F**) Front Hazcam (Hazard Avoidance Camera) image, 2F132673895FFL1900P1212L0M1, of Serpent, a 2-m bedform near the rim of Bonneville crater. (**G**) Pancam image, 2P131954281SFL1300P2531L7M1, of Terrace rock with ventifact grooves originating from a common horizon. (**H**) Pancam image, 2P133106987SFL2200P2567L2M1, of Mazatzal rock, showing prominent ventifact grooves. (**I**) Pancam image, 2P134272699FFL2500P2373L7M1, of two-toned rock. (**J**) Pancam image, 2P129999373FFL0506P2531R2M1, of Perched rock. (**K**) Pancam image, 2P129556193FFL0329P2580L2M1, of Adirondack and (**L**) Pancam image, 2P131696760EEF1159P2597L5M1, of Humphrey rock, showing the 4.5-cm areas abraded by the RAT and the distribution of the abraded cuttings (dark area) and the inferred wind direction (white arrow) at the time of abrasion.

Arena (Fig. 1, C, D, and E) show that the side with the lower slope (i.e., the windward side) has a crest that consists of a layer of well-sorted coarse particles (~1.8 mm in diameter) overlying finer grains, whereas the trough consists of a poorly sorted mixture of particles. These properties are characteristic of ripples on Earth (*21*, *22*). Although only one bedform has been imaged to date by the MI on both its inferred windward and leeward sides, we conclude that the smaller bedforms seen at the Spirit site are ripples (*22*).

Some of the rocks have associated triangular-shaped deposits of regolith, similar to those seen at previous landing sites on Mars, termed wind tails. The wind tails tend to scale with the size of the rock with which they are associated, and at the MPF site the orientation of the tapered part of the wind tail is considered to point in the downwind direction (*23*, *24*). However, unlike the MPF site, many of the drift deposits around the rocks at Gusev have a layer of coarse particles that form an armored surface, similar to the debris aprons described above.

The wheels on Spirit were used to dig into regolith deposits (*9*), which revealed the presence of a surface crust and poorly sorted particles. We suggest that the larger grains of debris aprons, drift deposits, and ripples have been concentrated on the surface as a lag through the winnowing action of the wind that has removed the finer sand and dust. The coarse grains on the ripple crests are further concentrated by saltation impact, typical of ripple formation on Earth. This winnowing can lead to size-sorted bedding structures.

We observed an increase in rock size and frequency around Bonneville crater, reflecting ejecta that was thrown out of the crater during an impact event (*25*). There is a corresponding increase in drift deposits around Bonneville (Fig. 1F), which we attribute to the increase in surface roughness. Although overall wind shear stress increases when wind encounters rougher terrain (*26*, *27*), the fraction of the shear stress available for mobilizing particles decreases, reducing the surface flux of particles and leading to net deposition (*28*, *29*). There is also an increase in the proportion of rocks for which the tops are dust-mantled. We attribute this to the rover traverse passing out of the recent dust devil track that cuts across the landing zone and into an area that has not been swept clean by a recent dust devil (Fig. 1A).

Many of the rocks at the Columbia Memorial Station have flat faces (facets) and/or grooves cut into their surfaces, giving them the appearance of wind-abraded rocks, or ventifacts. The facets form beveled surfaces inclined 20° to 70° from the horizontal. The grooves range in size from 2 to 50 cm long by 0.5 to 5 cm wide and occur on the facets and on irregular surfaces. Most of the facets and grooves are on the northwest sides of the rocks. Although they are similar in morphology to rocks seen at the MPF site (*30*), they are less common at the Spirit site.

Terrace rock (Fig. 1G) has a zone of ventifact grooves that originates at a horizon a few cm above the ground. A similar zone is seen on a smaller rock nearby. This horizon could represent a change in the properties of the rock (in which the lower part is more resistant to abrasion), a horizontal fracture in the rock that served as an initiation zone for abrasion, or an indication that the lower part of the rock was buried and shielded from abrasion. Mazatzal (Fig. 1H) is a light-toned, flat rock with ventifact grooves cut into the upper surface. We suggest that the prominent grooves resulted from the trajectories of abrading particles that struck the rock at low angles, gouging the surface, an interpretation consistent with laboratory experiments of rock abrasion under martian conditions (*31*, *32*).

The regolith beneath some rocks has been removed, giving the rock an undercut appearance. Many of the low-lying flat rocks are partly buried in the regolith and have bright, dusty surfaces (*11*). In other cases, rocks are two-toned: the lower part of the rock is bright and the tops of the rocks are darker and less dusty (Fig. 1I).

In a few cases along the traverse, Spirit imaged rocks that are perched on top of other rocks (Fig. 1J). These could be (i) inclusions or fragments released by weathering from a single rock, (ii) fragments emplaced as impact ejecta, or (iii) the remnant of a former mantling deposit where the finer-grained material has been mostly removed, with the perched rock having sunk into place.

The Rock Abrasion Tool (RAT) is used to abrade and brush the surface of rocks for analyses (*33*). Premission experiments demonstrated that in the absence of winds the brush disperses cuttings in symmetrical trajectories radially from the abrasion area. In the presence of wind, the material is carried downwind, leaving an asymmetric pattern. Two rocks at the Spirit site, Adirondack and Humphrey, were abraded, and in the process the abraded debris was distributed asymmetrically from the abraded area. Grinding operations took place for 3 hours starting at 12:30 hours local solar time (LST) for Adirondack and for 4 hours starting at 11:30 hours LST for Humphrey. We interpret the pattern of RAT cuttings (Fig. 1, K and L) to indicate that wind was actively blowing from the northwest toward the southeast in both cases. The asymmetry is more prominent on Adirondack, suggesting higher wind speeds.

Before Spirit landed, wind regimes were predicted from mesoscale atmospheric models (*33*, *34*) and from analyses of features seen from orbit (*36*). These studies suggested that strong winds occur in the afternoon at Gusev Crater, coincident with the strongest heating of the atmosphere, and that wind orientations are about radial from the central zone of the crater. In the landing area, the predicted prevailing winds are from the north-northwest toward the south-southeast, which is along the axis of the dust devil tracks seen from orbit. At night, the winds in the area reverse direction, a result of cold air ponding in the crater.

The asymmetric distribution of the RAT cuttings are consistent with predicted afternoon winds from the northwest. Moreover, the orientations of the axes of most of the bedforms (e.g., ripples) observed from Spirit are east-northeast to the west-southwest. On the assumption that these features are ripples, their axes would be orthogonal to the winds, which could be either from the northwest or from the southeast. However, the slight asymmetry of some bedforms (with steeper faces on the southeast) suggests prevailing winds from the north-northwest on the assumption that the steep side is the slip face. The observation that the asymmetry is not pronounced could reflect the day-to-night reversing winds. The wind-abraded grooves and facets are predominantly on the northwest sides of the rocks, also consistent with winds from that direction. These features also suggest that wind abrasion resulted from winds capable of transporting particles that were derived from sources northwest of the site.

A fundamental issue is the current activity of windblown particles on Mars and at the Gusev site. Frequent observations of martian dust storms, changes in dust devil tracks at the Spirit site, and accumulated dust on the rover demonstrate that fine particles are currently entrained, transported, and deposited by the wind. However, no bedform on Mars has been seen to change size, shape, or position from either orbit or the surface. MI images of the surfaces and interiors of regolith patches and bedforms show that most of the deposits consist of poorly sorted mixtures of different grain sizes and that many of the regoliths and bedform surfaces are crusted by a thin layer (*9*). If the coarse grains were undergoing active saltation, the dust and finer materials should have been removed by wind winnowing. Moreover, the ventifacted rock surfaces are mantled with dust and possibly a weathering rind (*9*), and if grains were undergoing active saltation they should be swept clean of dust by impacts. On the basis of these observations, it is unlikely that grains other than dust are currently being transported by wind at the landing site.

Undercut rocks, perched rocks, and other features discussed above suggest that the surface within Gusev Crater has been lowered over time. We infer, for example, that the bright zone of the two-toned rocks represents the buried part, similar to two-toned rocks seen in deserts on Earth and at the MPF site (*23*, *24*). Burial could have occurred as part of a widespread deposit or by the passage of a bedform, such as a dune. If all of these features are the result of widespread deflation, measurements of the undercut rocks, the height to the boundary between the bright and

dark parts of the two-toned rocks, the height of the largest of the bright (light-toned) rocks, and the perched rocks would suggest local deflation of 5 to 60 cm. Thus, there must have been previous deposition on this order.

References and Notes

1. Reviewed by R. Greeley, N. Lancaster, S. Lee, P. Thomas, in *Mars*, H. H. Kieffer, B. Jakosky, Eds. (Univ. of Arizona Press, Tucson, AZ, 1992), pp. 730–766.
2. S. W. Squyres *et al*., *Science* **305**, 794 (2004).
3. J. A. Crisp *et al*., *J. Geophys. Res.* **108**, 10.1029/2002JE002038 (2003).
4. M. P. Golombek *et al*., *J. Geophys. Res.* **108**, 10.1029/2003JE002074 (2003).
5. M. P. Golombek *et al*., *Lunar Planet. Sci.* **XXXV**, abstr. 2185 (2004).
6. At 0.19 (*36*), the landing site has the lowest albedo as determined from orbit of the entire landing ellipse. From analysis of broadband (0.4 to 1.0 μm) images from the MER Pancam; the average albedo measured from the surface is 0.25 ± 0.05 (*10*).
7. A martian solar day has a mean period of 24 hours 39 min 35.244 s and is referred to as a sol to distinguish this from a roughly 3% shorter solar day on Earth. A martian sidereal day, as measured with respect to the fixed stars, is 24 hours 37 min 22.663 s, as compared with 23 hours 56 min 04.0905 s for Earth. See www.giss.nasa.gov/tools/mars24/ for more information.
8. "Dust" is an imprecise term but is commonly used for material on Earth that is smaller than about 40 μm and that is transported primarily in suspension. Estimates for dust on Mars suggest diameters of a few micrometers, although these particles are thought to stick together in some cases, possibly by electrostatic charges, to form aggregates of larger sizes (*37*).
9. R. E. Arvidson *et al*., *Science* **305**, 821 (2004).
10. Names have been assigned to areographic features by the Mars Exploration Rover (MER) team for planning and operations purposes. The names are not formally recognized by the International Astronomical Union.
11. J. F. Bell III *et al*., *Science* **305**, 800 (2004).
12. K. E. Herkenhoff *et al*., *J. Geophys. Res.* **108**, 10.1029/2003JE002076 (2003).
13. J. B. Pollack *et al*., *J. Geophys. Res.* **82**, 4479 (1977).
14. P. H. Smith *et al*., *Science* **278**, 1758 (1997).
15. M. G. Tomasko, L. R. Doose, M. Lemmon, P. H. Smith, E. Wegryn, *J. Geophys. Res.* **104**, 8987 (1999).
16. P. R. Christensen *et al*., *Science* **305**, 837 (2004).
17. H. Y. McSween *et al*., *Science* **305**, 842 (2004).
18. K. E. Herkenhoff *et al*., *Science* **305**, 824 (2004).
19. J. F. Bell *et al*., *Icarus* **158**, 56 (2002).
20. J. L. Bandfield, *J. Geophys. Res.* **107**, 10.1029/2001JE001510 (2002).
21. R. P. Sharp, *J. Geol.* **71**, 617 (1963).
22. Ripples are bedforms composed of sand and granules that are moved by surface creep induced by the impact of saltating sands, whereas dunes are larger bedforms typically composed of finer sands and not formed directly by saltation processes.
23. R. Greeley *et al*., *J. Geophys. Res.* **104**, 8573 (1999).
24. M. P. Golombek, N. T. Bridges, *J. Geophys. Res.* **105**, 1841 (2000).
25. J. A. Grant *et al*., *Science* **305**, 807 (2004).
26. R. Greeley, J. D. Iversen, *Wind as a Geological Process: Earth, Mars, Venus, and Titan* (Cambridge Univ. Press, Cambridge, 1985).
27. R. Greeley, J. D. Iversen, *Geophys. Res. Lett.* **14**, 925 (1987).
28. M. R. Raupach, *Boundary-Layer Meterol.* **60**, 375 (1992).
29. M. R. Raupach, D. A. Gillette, J. F. Leyes, *J. Geophys. Res.* **98**, 3023 (1993).
30. N. T. Bridges *et al*., *J. Geophys. Res.* **104**, 8595 (1999).
31. R. Greeley *et al*., *J. Geophys. Res.* **87**, 10009 (1992).
32. N. T. Bridges *et al*., *Planet. Space Sci.* **52**, 199 (2004).
33. S. P. Gorevan *et al*., *J. Geophys. Res.* **108**, 10.1029/2003JE002061 (2003).
34. S. R. C. Rafkin, T. I. Michaels, *J. Geophys. Res.* **108**, 10.1029/2002JE002027 (2003).
35. D. Toigo, M. I. Richardson, *J. Geophys. Res.* **108**, 10.1029/2003JE002064 (2003).
36. R. Greeley *et al*., *J. Geophys. Res.* **108**, 10.1029/2002JE002006 (2003).
37. M. T. Mellon, B. M. Jakosky, H. H. Kieffer, P. R. Christensen, *Icarus* **148**, 437 (2000).
38. R. Greeley, *J. Geophys. Res.* **84**, 6248 (1979).

39. Our work was supported by NASA by contracts through the Jet Propulsion Laboratory.

10 May 2004; accepted 23 June 2004

REPORT

Localization and Physical Properties Experiments Conducted by Spirit at Gusev Crater

R. E. Arvidson,[1] R. C. Anderson,[2] P. Bartlett,[3] J. F. Bell III,[4] D. Blaney,[2] P. R. Christensen,[5] P. Chu,[3] L. Crumpler,[6] K. Davis,[3] B. L. Ehlmann,[1] R. Fergason,[5] M. P. Golombek,[2] S. Gorevan,[3] J. A. Grant,[7] R. Greeley,[5] E. A. Guinness,[1] A. F. C. Haldemann,[2] K. Herkenhoff,[8] J. Johnson,[8] G. Landis,[9] R. Li,[10] R. Lindemann,[2] H. McSween,[11] D. W. Ming,[12] T. Myrick,[3] L. Richter,[13] F. P. Seelos IV,[1] S. W. Squyres,[4] R. J. Sullivan,[4] A. Wang,[1] J. Wilson[3]

The precise location and relative elevation of Spirit during its traverses from the Columbia Memorial station to Bonneville crater were determined with bundle-adjusted retrievals from rover wheel turns, suspension and tilt angles, and overlapping images. Physical properties experiments show a decrease of 0.2% per Mars solar day in solar cell output resulting from deposition of airborne dust, cohesive soil-like deposits in plains and hollows, bright and dark rock coatings, and relatively weak volcanic rocks of basaltic composition. Volcanic, impact, aeolian, and water-related processes produced the encountered landforms and materials.

During the first few Mars solar days (sols) (*1*) of operations, we determined the landed location in inertial coordinates by analyzing Spirit-to-Earth two-way X-band Doppler transmissions and two passes of ultrahigh-frequency two-way Doppler between Spirit and the Mars Odyssey orbiter. The equivalent location in the International Astronomical Union (IAU) 2000 body-centered reference frame is 14.571892°S, 175.47848°E. The location with respect to surface features was derived by the correlation of hills and craters observed in images taken by the Pancam, the Entry Descent and Landing (EDL) Camera, and the Mars Orbital Camera. On the basis of these analyses, the landing site is located at 14.5692°S, 175.4729°E in IAU 2000 coordinates, ~300 m north-northwest of the radiometric solution. This offset is consistent with the map tie errors between inertially derived coordinate systems and those derived from image-based coverage of the planet.

Localization experiments during traverses focused on systematic acquisition of forward- and backward-looking overlapping images, onboard inertial measurement unit (IMU) observations to derive rover tilt, and tracking the number of wheel turns to provide wheel-based odometry. These observations were employed in a least-squares bundle adjustment to solve for the position and orientation of Spirit in local Cartesian coordinates at discrete locations during traverses (Fig. 1 and Plate 14). In addition, measurements of differential rocker and bogie angles in the suspension system, together with IMU data, were used to reconstruct the elevation of each wheel at a 2- to 8-Hz sample rate relative to the start of each traverse (Fig. 1).

Localization results were extracted for 33 traverse segments from the Columbia Memori-

[1]Department of Earth and Planetary Sciences, Washington University, St. Louis, MO 63130, USA. [2]Jet Propulsion Laboratory, California Institute of Technology, Pasadena, CA 91109, USA. [3]Honeybee Robotics, 204 Elizabeth Street, New York, NY 10012, USA. [4]Department of Astronomy, Space Sciences Building, Cornell University, Ithaca, NY 14853, USA. [5]Department of Geological Sciences, Arizona State University, Tempe, AZ 85287, USA. [6]New Mexico Museum of Natural History and Science, Albuquerque, NM 87104, USA. [7]Center for Earth and Planetary Studies, National Air and Space Museum, Smithsonian Institution, Washington, DC 20560, USA. [8]U.S. Geological Survey, Flagstaff, AZ 86001, USA. [9]National Aeronautics and Space Administration (NASA) Glenn Research Center, Cleveland, OH 44135, USA. [10]Department of Civil and Environmental Engineering and Geodetic Science, Ohio State University, Columbus, OH 43210, USA. [11]Department of Earth and Planetary Sciences, University of Tennessee, Knoxville, TN 37996, USA. [12]NASA Johnson Space Center, Houston, TX 77058, USA. [13]Deutsche Luft und Raumfahrt Institut für Raumsimulation, Linder Hoehe, Koln, DJ-51170, Germany.